Advances in Materials Research, *Vol. 14, No. 3 (2025) 249-268*
https://doi.org/10.12989/amr.2025.14.3.249

Thermo-mechanical stress and deformation analysis of functionally graded cylinder subjected to multiple loading conditions

Sanjay Kumar Singh[1], Lakshman Sondhi[2], Anil Prakash Singh[3], Rakesh Kumar Sahu[4] and Royal Madan[5*]

[1]*Department of Mechanical Engineering, Chhatrapati Shivaji Institute of Technology Durg*
[2]*Department of Mechanical Engineering, Shri Shankaracharya Technical Campus Bhilai*
[3]*Maharana Pratap Polytechnic, Gorakhpur, 273015*
[4]*Department of Mechanical Engineering, Visvesvaraya National Institute of Technology, Nagpur*
[5]*Department of Mechanical Engineering, Graphic Era (Deemed to be University), Dehradun 248002, Uttarakhand, India*

(*Received February 22, 2025, Revised June 29, 2025, Accepted July 1, 2025*)

Abstract. In this paper, thermo-mechanical elastic stress and deformation analysis of a functionally graded (FG) cylindrical shell, under complex loading states such as angular rotation, thermal load with heat generation, body force, and mechanical loads, are analyzed. FG materials are advanced and futuristic composite materials with gradually varying properties across different surfaces. In this paper, a power law is used for the variation of material properties such as elastic modulus, density, thermal conduction coefficient, and thermal expansion coefficient, offering a better strength-to-weight ratio, better thermal resistance, and durability in critical harsh environments. To increase the lifecycle of a structure, the stresses induced should be minimal. Navier's method is used to solve Euler's governing differential equations with a plane stress condition that reduces the complexity of the second-order. The main aim of this study is to investigate the combined effect of material non-homogeneity with various types of complex loading states on the displacement and stress distribution within the cylinder. This analysis provides valuable insight to enhance the performance, reliability, and integrity of structures in the fields of aerospace, defense, Mechanical, and Civil Engineering.

Keywords: FGM; hollow cylinder; material grading laws; Navier's method; thermo-mechanical analysis

1. Introduction

Functionally graded materials are advanced materials whose mechanical and physical properties are graded in a specific direction. The structure includes beams, shafts, cylinders, and plates with many industrial applications (Birman and Kardomateas 2018, Bouakkaz *et al*. 2024, Namayandeh *et al*. 2020, Nikbakht *et al*. 2019). The smooth variation of material properties can be tailored as per the requirements that can meet the needs of various industrial applications (Adiga *et al*. 2022, Boss and Ganesh 2006). This gradual change in microstructure across the interface does not mismatch the mechanical properties across the multiple interfaces as other composite materials, such as laminated

*Corresponding author, Ph.D., E-mail: royalmadan.me@geu.ac.in; royalmadan6293@gmail.com

http://www.techno-press.org/?journal=amr&subpage=5 ISSN: 2234-0912 (Print), 2234-179X (Online)

reinforced, do (Nakamura *et al.* 2000). Such changes in stepwise or continuous gradation in the material are a result of the fabrication process. The step-wise layered FGM can be developed using powder metallurgy or additive manufacturing while a continuous variation in properties can be achieved using the centrifugal casting method (Madan and Bhowmick 2020, Suresh and Mortensen 1997). Unlike laminated composites, which may exhibit abrupt changes in mechanical properties at the interface.

FGMs provide a gradual variation in microstructure, reducing property mismatches across the interface (Daneshmand *et al.* 2023, Raad *et al.* 2024). Non-linear free vibration analysis of simply supported FGM plate was performed, and the partial differential equations (PDE) were determined according to first-order shear deformation theory (FSDT) (Hashemi and Jafari 2020). Employed first-order shear deformation theory to examine the free vibration behavior of eccentrically stiffened functionally graded materials (ES-FGM) of simply supported shallow shells subject to thermo-mechanical loads (Kumar and Kumar 2021). Adopted an analytical method by using the Rayleigh-Ritz technique and sinusoidal shear deformation theory to analyze the performance of free vibration of porous functionally graded circular cylindrical shells with different boundary conditions (Wang and Wu 2017). Improved Donnell nonlinear shell theory to investigate the free vibration of metal foam circular shells strengthened with graphene platelets (Wang and Zhao 2019). A problem of thermal buckling of FG porous rectangular plate using Navier's method was solved and the influence of critical buckling temperature was investigated (Ellali *et al.* 2024). A semi-analytical solution to study the bending that occurs in the rotating disks formed of the functionally graded material (FGM) under different boundary conditions was carried out. They found stresses induced in an isotropic material to be higher than stresses induced in an FG disk (Bayat *et al.* 2009). In (Wang *et al.* 2015), discussed the thermo-mechanical stress analysis of FGM pressure vessels for a steady-state thermo-elastic theory by considering power law material gradation. Bending analysis of FG curved sandwich beams under uniform mechanical load was performed using higher-order shear deformation theory (HSDT) (Draiche *et al.* 2021). Furthermore, a static and dynamic analysis of the FG doubly curved shell structure was performed for a power law variation of material properties under a simply supported boundary condition (Draiche *et al.* 2024). Performed bending and free vibration analysis on FG sandwich plate and shells by employing HSDT and refined HSDT (Allam *et al.* 2020, Zine *et al.* 2018). A free vibration analysis of functionally graded CNTRC beams using variational methods and a 3-9-1 ANN model was carried out using Eringen's nonlocal theory, and ANN (Madenci Emrah *et al.* 2024)

A problem of stresses induced in an FG hollow cylinder, disk, and sphere under internal pressure is solved using the complementary functions method (Tutuncu and Temel 2009). Furthermore, for an FG cylinder under different loading conditions problem, an analytical solution is presented (Rahimi *et al.* 2011). For a short hollow cylinder under a steady-state thermal load stresses are identified analytically (Jabbari *et al.* 2009). Elastic analysis of a thick hollow cylinder of variable thickness under arbitrary pressure at the inner surface was performed using finite element analysis (Nejad *et al.* 2015). Material modeling of composites and FGMs can be carried out by methods such as rule of mixture, modified rule of mixture, Mori-Tanaka and Halpin-Tsai, (Hadji *et al.* 2021, Kadum Njim *et al.* 2024, Sondhi *et al.* 2023) etc. The models consider the individual composition of two phases, which can be a combination of metal-ceramic, ceramic-ceramic, metal-metal, or polymers, etc. The other approach considers the direct variation of material properties by varying it exponentially (Garg *et al.* 2024), power law (Madan *et al.* 2020, Rabia *et al.* 2024), trigonometric laws (Madan and Bhowmick 2022), etc. Based on these theories, in one of the studies, a Mori-Tanaka-based material model was utilized to study a 2D FG thick hollow cylinder (Najibi and

Shojaeefard 2016). Apart from these different methodologies have been adopted by many researchers in solving the problem of thick cylinders which are a mesh-free method (Mahmoud Hosseini 2014), shear deformation theory (Rahimi *et al*. 2012), Navier's method (Dai and Fu 2006, Safari *et al*. 2011), elasticity method (Tutuncu and Temel 2009) and analytical methods (Alhous *et al*. 2025, Al-Shablle *et al*. 2023, Kadum Njim *et al*. 2024, Abbas *et al*. 2025) etc.

The present study contributes to the analytical modeling and analysis of FG cylindrical vessels under complex loading conditions. Despite extensive literature, no research has been conducted that proposes an analytical approach to the thermo-mechanical deformation and stress analysis of FGM cylindrical vessels subjected to various angular rotations, body forces, mechanical loads (internal and external pressure), and thermal load with heat generation. Additionally, the present study examines stress and deformation behavior under real-life complex loading conditions, analyzing the effects of material parameters following a power-law variation, as well as thermal and mechanical loading parameters along with body force. Navier's method is employed to solve the second-order governing differential equation, demonstrating its robustness in handling such a combination of loads. Importantly, this work uniquely considers the combined effect of various realistic complex loading conditions. Such a multi-physics and multi-parameter analytical approach is rarely addressed in existing literature, especially for a closed-form solution. Additionally, parametric studies presented in this paper offer insights into the influence of the material gradation parameter and thermo-mechanical loading variables on stress and displacement distributions, which are crucial for the design optimization of critical components of aerospace, defense, mechanical, and civil engineering systems.

2. Mathematical formulation

Considering a hollow cylindrical geometry made of FG material with inner radius '$\boldsymbol{a}$', and outer radius '$\boldsymbol{b}$' as shown in Fig. 1. Let the displacement 'u' be the function of the radius of a cylinder. The radial strain, tangential strain, and displacement are related to Eq. 1 (Jabbari *et al*. 2002)

$$\varepsilon_{rr} = \frac{du}{dr} = \frac{1}{Y_{rr}}[\sigma_{rr} - \vartheta\sigma_{tt}] + {\varepsilon_{tt}}^{*}\,,\ \varepsilon_{tt} = \frac{u}{r} = \frac{1}{Y_{rr}}[\sigma_{tt} - \vartheta\sigma_{rr}] + {\varepsilon_{tt}}^{*}\,,\ {\varepsilon_{tt}}^{*} = \alpha_{rr}T_{rr} \qquad (1)$$

The plane stress state is considered for reducing the complexity of the analysis, in the plane stress condition the thickness of the cylinder wall is very thin as compared to the radius due to this assumption plane stress components are neglected.

For elastic materials, the thermo-mechanical stress-strain relations for non-homogeneous and isotropic materials under the influence of temperature are given by Hooke's law (Jabbari *et al*. 2002).

$$\sigma_{rr} = Y_{rr}\lambda[\varepsilon_{rr}(1-\vartheta) + \vartheta\varepsilon_{tt} - (1+\vartheta){\varepsilon_{rr}}^{*}]\,,\ \sigma_{tt} = Y_{rr}\lambda[\vartheta\varepsilon_{rr} + (1-\vartheta)\varepsilon_{tt} - (1+\vartheta){\varepsilon_{rr}}^{*}] \quad (2)$$

where, σ_{rr}, σ_{tt} represents the radial and tangential stress and ε_{rr}, ε_{tt} represents the radial and tangential strain respectively. The α_{rr}, T_{rr} represents the coefficient of thermal expansion (CTE) and change in temperature profile along the radius of the cylinder and ϑ is considered as the constant Poisson's ratio.

Eq. 3 shows the governing equilibrium equation expressed by Navier's equation for the plane stress including the body force and the inertia term in the radial direction. The basic unknown parameter is the displacement at each discretised point along the thickness of the cylinder.

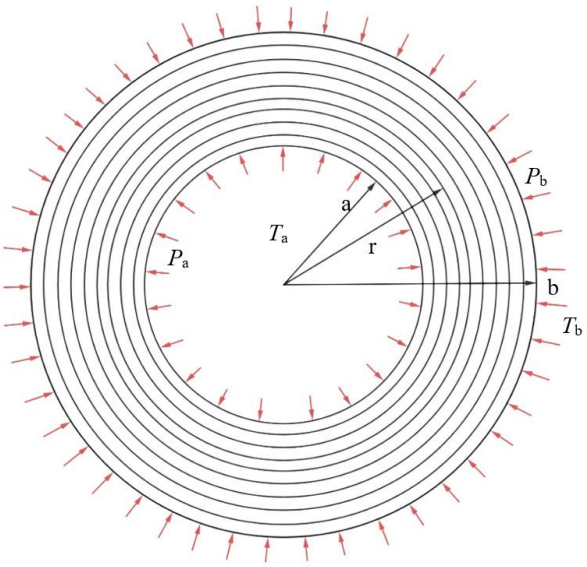

Fig. 1 FGM cylinder

$$r\frac{d}{dr}\sigma_{rr} + (\sigma_{rr} - \sigma_{t_t}) + \rho_{rr}\left(\omega^2 - \frac{g}{a}\right)r^2 = 0 \tag{3}$$

where, ω, g and ρ_{rr} denotes the rotation and gravity and density of a material,

The material gradation is controlled and established using chemical vapour deposition, powder metallurgy, or centrifugal casting. The material properties vary according to power-law was considered as (Jabbari *et al*. 2002). Young's modulus Y_{rr}, CTE, α_{rr}, thermal conductivity k_{rr}, density ρ_{rr} and heat flux q_{rr} are assumed to vary as follows:

$$Y_{rr} = Y_0(r)^{m_1}; \alpha_{rr} = \alpha_0(r)^{m_2}; \rho_{rr} = \rho_0(r)^{m_4} \rho_{rr} = \rho_0(r)^{m_4} m,\ q_{rr} = q_0(r)^{m_5} \tag{4}$$

where Y_0, α_0, k_0, $\rho_{0,}$, q_0 are Young's modulus, CTE, thermal conductivity, density, and heat flux properties for the homogeneous cylinder or the same at the inner surface for all FG profiles respectively. And m_1, m_2, m_3, m_4, m_5 are the material inhomogeneity constant on the basis of which a cylinder is functionally graded radially.

To solve the governing equation, the first strains that are a function of displacement as in Eq. 1 are substituted in the stress-strain relation as in Eq. 2 which illustrates the stress as the function of displacement. The obtained results are then substituted in governing differential Eq. 3. Finally, the Navier equation in the form of displacement is attained as:

$$\begin{aligned} &r\frac{d}{dr}\left[Y_{rr}\lambda\left\{\vartheta\frac{u}{r} + (1-\vartheta)\frac{du}{dr} - (1+\vartheta)\varepsilon_{rr}{}^*\right\}\right] + Y_{rr}\lambda\left[\vartheta\frac{u}{r} + (1-\vartheta)\frac{du}{dr} - (1+\vartheta)\varepsilon_{rr}{}^*\right] \\ &-Y_{rr}\lambda\left[(1-\vartheta)\frac{u}{r} + \vartheta\frac{du}{dr} - (1+\vartheta)\varepsilon_{rr}{}^*\right] + \rho_{rr}(\omega^2 - \frac{g}{a})r^2 = 0 \end{aligned} \tag{5}$$

where λ defines the material parameter and is given by:

$$\lambda = \frac{1}{(1+\vartheta)(1-2\vartheta)} \tag{6}$$

For ease of the calculation, Eq. (5) can be rewritten and converted into standard differential equation form and introducing some arbitrary constants as,

$$A_1 r^2\left(\frac{d^2u}{dr^2}\right)+A_2 r\left(\frac{du}{dr}\right)+A_3(u)=A_4 r^{m_2+P_4+1}+A_5 r^{m_2-m_3+m_5+3}+A_6 r^{m_2+1}+A_7 r^{m_4-m_1+3} \tag{7}$$

where arbitrary constants are given by,

$$\begin{gathered} A_1=Y_0\lambda(1-\vartheta),\ A_2=Y_0\lambda[m_1(1-\vartheta)+(1-\vartheta)] \\ A_3=Y_0\lambda\left(\vartheta m_1+\vartheta-1\right);A_4=\frac{1}{\left(1-2\vartheta\right)}Y_0\alpha_0 Q_4\left[P_4+m_1+m_2\right] \\ A_5=\frac{\beta_1 Y_0\alpha_0}{(1-2\vartheta)}[m_5-m_3+m_1+m_2+2],\ A_6=\frac{Y_0\alpha_0 Q_3}{(1-2\vartheta)}[m_1+m_2],\ A_7=-\rho_0\left[\omega^2-\left(\frac{g}{a}\right)\right] \end{gathered} \tag{8}$$

3. Temperature formulation

Assuming FG materials under high-temperature application and a combination of material properties will be chosen based on temperature. Temperature distribution of one-dimensional steady-state heat conduction equation with constant heat flux is governed by (Jabbari *et al*. 2002) with varying heat conductivity.

$$\frac{d}{dr}\left[rk_{rr}\frac{dT_{rr}}{dr}\right]=-rq_{rr} \tag{9}$$

The thermal boundary conditions employed at the inner and outer radius of a cylinder are given by,

$$T_{rr}|r=a=T_a \text{ and } T_{rr}|r=b=T_b \tag{10}$$

where, T_{rr} is the instantaneous temperature, the temperature at the inner and outer radius was defined by T_a & T_b.

Differentiating the above Eq. (9), the Navier equation for temperature can be rewritten as

$$M_1 r^2\left(\frac{d^2T_{rr}}{dr^2}\right)+M_2 r\left(\frac{dT_{rr}}{dr}\right)+M_3(T_{rr})=M_4 r^{m_5-m_3+2} \tag{11}$$

where M_i, i =1 to 4 are the arbitrary thermal constants as follows,

$$\begin{gathered} M_1=k_0\ , M_2=k_0(1+m_3),\ M_3=0,\ M_4=-q_0, \\ P_3=0, P_4=\left(\frac{M_1-M_2}{M_1}\right)=-m_3 \end{gathered} \tag{12}$$

where, P_3 and P_4 are the thermal parameters

$$\frac{dT_{rr}}{dr}=P_4 Q_4 r^{P_4-1}+\beta_1(m_5-m_3+2)r^{m_5-m_3+1} \tag{13}$$

$$T_{rr}=Q_3+Q_4 r^{P_4}+\beta_1 r^{m_5-m_3+2} \tag{14}$$

Solving for Q_3 and Q_4 yields

$$Q_3 = T_a - \beta_1 a^{m_5 - m_3 + 2} - Q_4 a^{P_4}$$
$$Q_4 = \frac{T_a - T_b}{a^{P_4} - b^{P_4}} - \frac{\beta_1 (a^{m_5 - m_3 + 2} - b^{m_5 - m_3 + 2})}{a^{P_4} - b^{P_4}} \tag{15}$$

4. Solution of displacement Navier Equation

The Navier's equation for radial displacement '***u'*** is given in Eq. 7, the aforementioned equation is a non-homogeneous Euler differential equation which is solved in 2 sections: (a) general solution (u_g) using homogeneous parts and, (b) particular solution using non-homogeneous part:

$$u_g = Q r^P \tag{16}$$

Substitute the above Eq. (16) In the homogeneous eq. (7)

$$A_1 P^2 + (A_2 - A_1) P + A_3 = 0 \tag{17}$$

The above Eq. (17) has 2 real roots P_1 and P_2, which are given by

$$P_{1,2} = \frac{(A_1 - A_2) \pm \sqrt{(A_2 - A_1)^2 - 4A_1 A_3}}{2A_1} \tag{18}$$

Thus, the general solution is

$$u_g(r) = Q_1 r^{P_1} + Q_2 r^{P_2} \tag{19}$$

$$u_p = B_1 r^{m_2 + P_4 + 1} + B_2 r^{m_2 - m_3 + m_5 + 3} + B_3 r^{m_2 + 1} + B_4 r^{m_4 - m_1 + 3} \tag{20}$$

Now particular part of solution u_p is assuming to have the form Substitute above Eq. (20) in eq. (7) then rearrange, we get,

$$\begin{aligned} &\begin{bmatrix} A_1(m_2 + P_4 + 1)(m_2 + P_4) + \\ A_2(m_2 + P_4 + 1) + A_3 \end{bmatrix} B_1 r^{m_2 + P_4 + 1} \\ &+ \begin{bmatrix} A_1(m_2 + m_5 - m_3 + 3)(m_2 + m_5 - m_3 + 2) \\ + A_2(m_2 + m_5 - m_3 + 3) + A_3 \end{bmatrix} B_2 r^{m_2 - m_3 + m_5 + 3} \\ &+ [A_1(m_2 + 1)m_2 + A_2(m_2 + 1) + A_3] B_3 r^{m_2 + 1} + \\ &\begin{bmatrix} A_1(m_4 - m_1 + 3)(m_4 - m_1 + 2) + \\ A_2(m_4 - m_1 + 3) + A_3 \end{bmatrix} B_4 r^{m_4 - m_1 + 3} \\ &= A_4 r^{m_2 + P_4 + 1} + A_5 r^{m_2 - m_3 + m_5 + 3} + A_6 r^{m_2 + 1} + A_7 r^{m_4 - m_1 + 3} \end{aligned} \tag{21}$$

Equating the coefficient of identical power, we have general solution and particular solution together is the complete solution of displacement,

$$u = u_g + u_p \tag{23}$$

Thus,

$$\begin{aligned} u = {} & Q_1 r^{P_1} + Q_2 r^{P_2} + B_1 r^{m_2 + P_4 + 1} + B_2 r^{m_2 + m_5 - m_3 + 3} \\ & + B_3 r^{m_2 + 1} + B_4 r^{m_2 - m_1 + 3} \end{aligned} \tag{24}$$

Substituting Eq. (24) in Eq. (1) & (2), the strains and stresses distributions are obtained as,

$$\varepsilon_{rr} = Q_1 P_1 r^{P_1-1} + Q_2 P_2 r^{P_2-1} + B_1(m_2 + P_4 + 1) r^{m_2+P_4+1} + B_2(m_2 - m_3 + m_5 + 3) r^{m_2-m_3+m_5+2} + B_3(m_2 + 1) r^{m_2} + B_4(m_4 - m_1 + 3) r^{m_4-m_1+2}$$

$$B_1 = \frac{A_4}{A_1[(m_2 + P_4 + 1)(m_2 + P_4)] + A_2[m_2 + P_4 + 1] + A_3}$$

$$B_2 = \frac{A_5}{\begin{bmatrix} A_1\{(m_2 + m_5 - m_3 + 3)(m_2 + m_5 - m_3 + 2)\} \\ + A_2(m_2 - m_3 + m_5 + 3) + A_3 \end{bmatrix}} \tag{25}$$

$$B_3 = \frac{A_6}{A_1[(m_2 + 1)(m_2)] + A_2[(m_2 + 1)] + A_3}$$

$$B_4 = \frac{A_7}{\begin{bmatrix} A_1[(m_4 - m_1 + 3)(m_4 - m_1 + 2)] \\ + A_2[(m_4 - m_1 + 3)] + A_3 \end{bmatrix}}$$

$$\varepsilon_{tt} = Q_1 r^{P_1-1} + Q_2 r^{P_2-1} + B_1 r^{m_2+P_4} + B_2 r^{m_2-m_3+m_5+2} + B_3 r^{m_2} + B_4 r^{m_4-m_1+2} \tag{26}$$

$$\sigma_{rr} = Y_0 \lambda \begin{bmatrix} Q_1 \eta_1 r^{m_1+P_1-1} + Q_2 \eta_2 r^{m_1+P_2-1} \\ + B_1 r^{m_1+m_2+P_4} \eta_3 + B_2 r^{m_1+m_2+m_5-m_3+2} \eta_4 \\ + B_3 r^{m_1+m_2} \eta_5 + B_4 r^{m_4+2} \eta_6 - \\ (1+\vartheta)\alpha_0 \begin{Bmatrix} Q_3 r^{m_1+m_2} + Q_4 r^{m_1+m_2+P_4} + \\ \beta_1 r^{m_1+m_2+m_5-m_3+2} \end{Bmatrix} \end{bmatrix}$$

where

$$\begin{aligned} \eta_1 &= \{(1-\vartheta)P_1 + \vartheta\} \\ \eta_2 &= \{(1-\vartheta)P_2 + \vartheta\} \\ \eta_3 &= \{(1-\vartheta)(m_2 + P_4 + 1) + \vartheta\} \\ \eta_4 &= \{(1-\vartheta)(m_2 + m_5 - m_3 + 3) + \vartheta\} \\ \eta_5 &= \{(1-\vartheta)(m_2 + 1) + \vartheta\} \\ \eta_6 &= \{(1-\vartheta)(m_4 - m_1 + 3) + \vartheta\} \end{aligned} \tag{27}$$

Q_1 and Q_2 are determined using the mechanical free-free boundary conditions, considering the internal pressure p_a and external pressure p_b

$$\sigma_{rr}|_{r=a} = -p_a \text{ and } \sigma_{rr}|_{r=b} = -p_b \tag{28}$$

substituting boundary condition Eq. (28) in Eq. (27), the constants Q_1 and Q_2 are found as,

$$Q_1 = \frac{\phi_{22} X - \phi_{12} Y}{\phi_{11}\phi_{22} - \phi_{12}\phi_{21}}, \qquad Q_2 = \frac{\phi_{11} Y - \phi_{21} X}{\phi_{11}\phi_{22} - \phi_{12}\phi_{21}} \tag{29}$$

where,

$$\phi_{11} = Y_0 \lambda [P_1(1-\nu) + \nu] a^{m_1+P_1-1} \tag{30}$$

$$\phi_{12} = Y_0\lambda[P_2(1-\nu)+\nu]a^{m_1+P_2-1}$$
$$\phi_{21} = Y_0\lambda[P_1(1-\nu)+\nu]b^{m_1+P_1-1}$$
$$\phi_{22} = Y_0\lambda[P_2(1-\nu)+\nu]b^{m_1+P_2-1}$$
$$X = -Z(a) - p_a \ , \quad Y = -Z(b) - p_b \tag{31}$$

$$Z(a) = Y_0\lambda\begin{bmatrix} Q_1\eta_1 a^{m_1+P_1-1} + Q_2\eta_2 a^{m_1+P_2-1} \\ +B_1 a^{m_1+m_2+P_4}\eta_3 + B_2 a^{m_1+m_2+m_5-m_3+2}\eta_4 \\ +B_3 a^{m_1+m_2}\eta_5 + B_4 a^{m_4+2}\eta_6 - \\ (1+\vartheta)\alpha_0\begin{Bmatrix} Q_3 a^{m_1+m_2} + Q_4 a^{m_1+m_2+P_4} + \\ \beta_1 a^{m_1+m_2+m_5-m_3+2} \end{Bmatrix} \end{bmatrix} \tag{32}$$

$$Z(b) = Y_0\lambda\begin{bmatrix} Q_1\eta_1 b^{m_1+P_1-1} + Q_2\eta_2 b^{m_1+P_2-1} \\ +B_1 b^{m_1+m_2+P_4}\eta_3 + B_2 b^{m_1+m_2+m_5-m_3+2}\eta_4 \\ +B_3 b^{m_1+m_2}\eta_5 + B_4 b^{m_4+2}\eta_6 - \\ (1+\vartheta)\alpha_0\begin{Bmatrix} Q_3 b^{m_1+m_2} + Q_4 b^{m_1+m_2+P_4} + \\ \beta_1 b^{m_1+m_2+m_5-m_3+2} \end{Bmatrix} \end{bmatrix} \tag{33}$$

5. Result and discussion

Thermo-mechanical stress analysis was carried out on functionally graded hollow cylindrical vessels subjected to varying thermal distribution. FGM-composed results are presented and assumed to be temperature-independent isotropic elastic material properties. The geometrical and mechanical properties are given in Table 1. Displacement, stress, and material properties along the radial direction of the cylinder are represented as dimensionless values to demonstrate the effect of FG material. The following dimensionless values were used for the presentation of numerical results:

$$P = \frac{P_{rr}}{P_0},\ \sigma_r{}^* = \frac{\sigma_{rr}}{\sigma_0},\ \sigma_\theta * = \frac{\sigma_{\theta\theta}}{\sigma_0},\ u^* = \frac{u}{b} \tag{34}$$

where, P is normalized load, $\sigma_r{}^*$ is normalized radial stress, $\boldsymbol{\sigma_\theta}*$ is normalized tangential stress, $\boldsymbol{u}^*$ is normalized displacement.

Fig. 2 represents the dimensionless elastic modulus, thermal expansion coefficient, thermal conduction coefficient, and density, where $m_1 = m_2 = m_3 = m_4 = n$ and $m_5 = 0$ for constant heat flux along the radius. The inhomogeneity constant shows the stiffness variation along the radius i.e., $n > 0$ means increasing the stiffness, and $n < 0$ means decreasing the stiffness in the radial direction. Whereas $n = 0$ shows the isotropic material properties.

Table 1 Material properties and boundary conditions

Geometrical properties		Material properties						Boundary condition			
a	b	Y_0	α_0	k_0	ρ_0	q_0	ϑ	P_a	P_b	T_a	T_b
m	m	GPa	$per\ ^0C$	W/mk	kg/m^3	kj/m^3		MPa	MPa	^0C	^0C
1	1.2	200	$1.2*10^{-6}$	15	7800	$50*10^3$	0.3	50	0	10	0

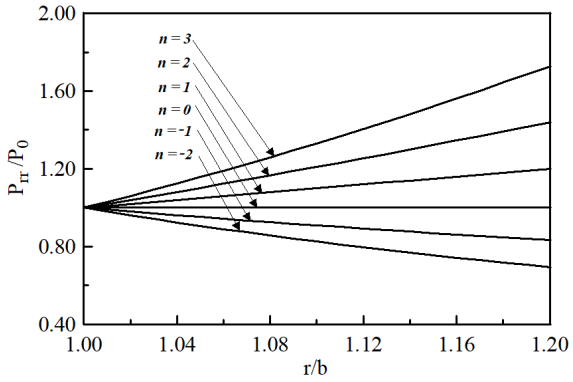

Fig. 2 Variation of material properties along the cylinder thickness with respect to the material parameter

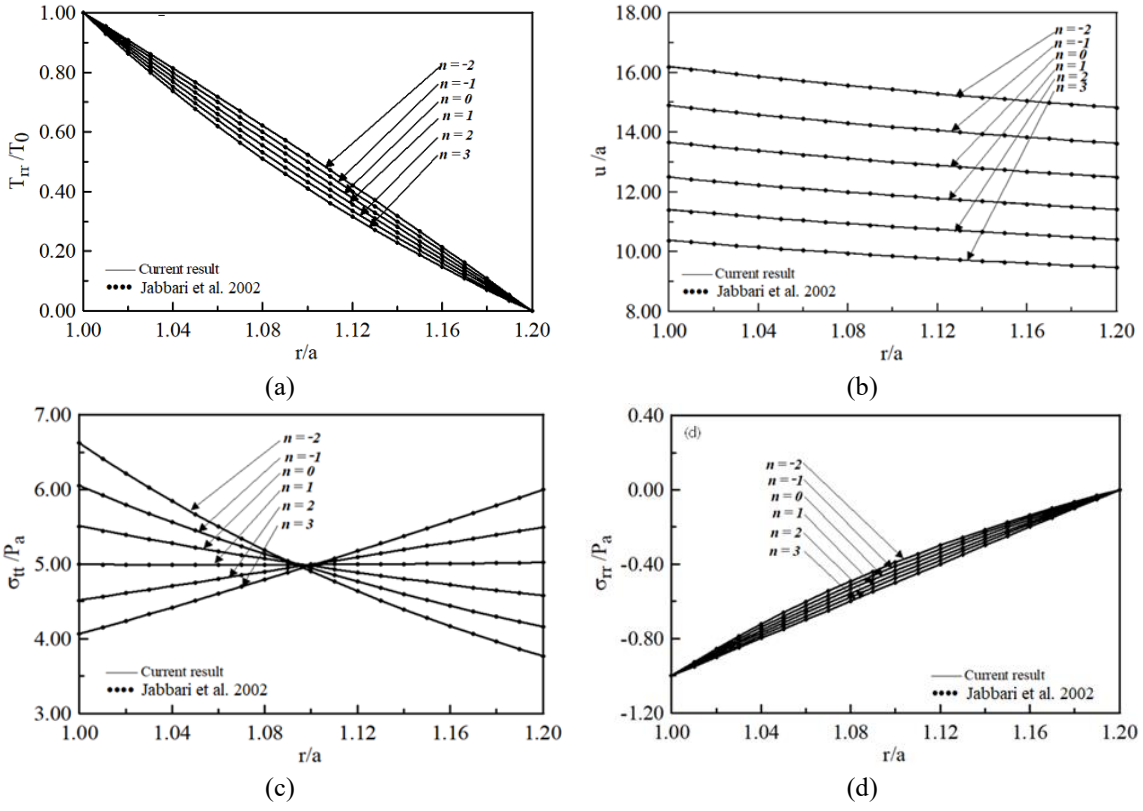

Fig. 3 Validation plot

5.1 Validation of the present study

Present results were validated with Reference (Jabbari *et al*. 2002) to check the feasibility of the methodology, which is illustrated in Fig. 3(a-d). Illustrated figures show excellent agreement with the published literature. For the effective stress analysis, the von Mises stress distribution $\sigma* = \sqrt{2}|\sigma_{rr} - \sigma_{tt}|$ is analyzed for all cases.

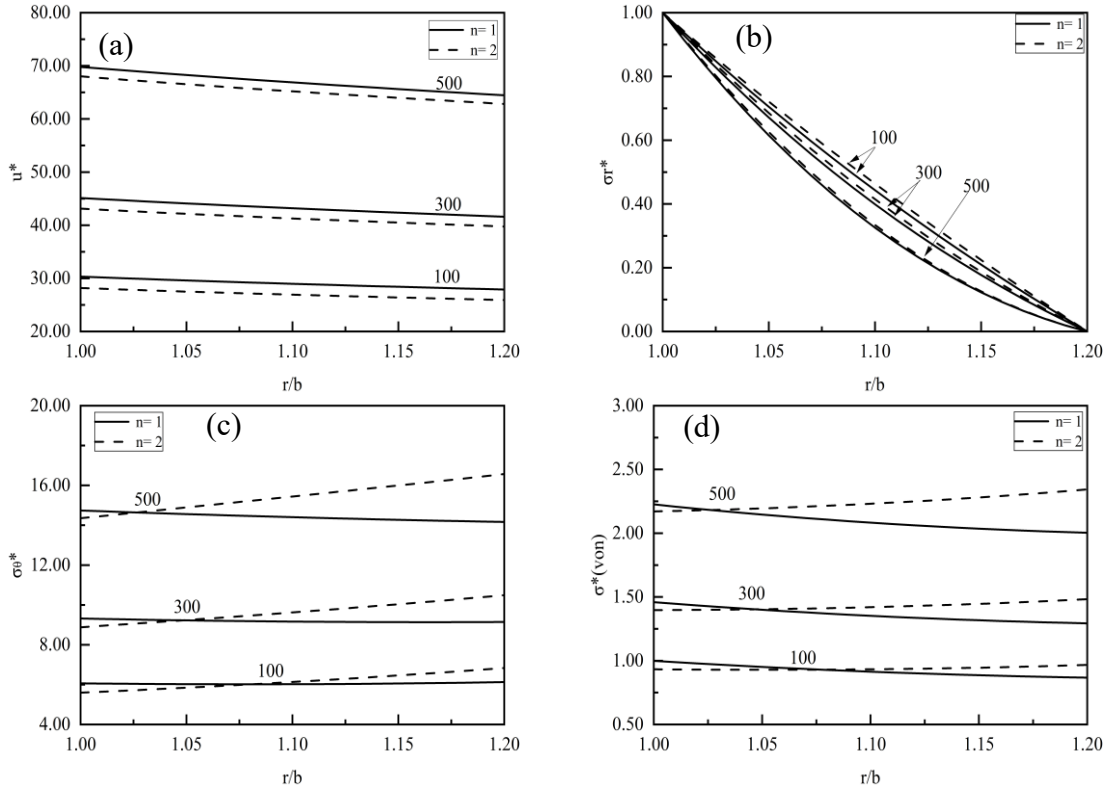

Fig. 4 Effect of various rotations on displacement and stresses for internal pressure case

5.2 Effect of various rotations (internal pressure)

Fig. 4(a-d) illustrates the effect of various rotations (100, 300, 500 rps) on displacement, radial stress, tangential stress, and von Mises stress, respectively, for an internally pressurized (50 MPa) cylinder. The magnitude of displacement, radial stress, and tangential stress is proportional to the rotation for both ***n*** = 1 & 2 throughout the thickness of the cylinder because angular rotation is proportional to the centrifugal force. But the magnitude of radial stress is inverse to the rotation throughout the thickness of the cylinder, which follows the boundary condition as shown, because the inner region resists internal pressure, experiencing compressive radial stress, while at the outer region, tensile stress is generated, which is the dominating stress. The variation in von Mises stress is primarily influenced by tangential stress, as evident from the results. Additionally, the effect of ***n*** is clearly observed in the figure. However, the critical value of ***n*** concerning the cylinder's radius is distinctly noticeable only in the tangential stress and von Mises stress distribution graphs, which shift toward the inner radius as the angular speed increases. For accurate prediction of failure, it is essential to thoroughly understand the stress variation with varying angular rotation & material properties.

5.3 Effect of various temperature (internal pressure)

Fig. 5(a-d) shows the effect of various temperatures (100, 200, 400) on displacement, radial

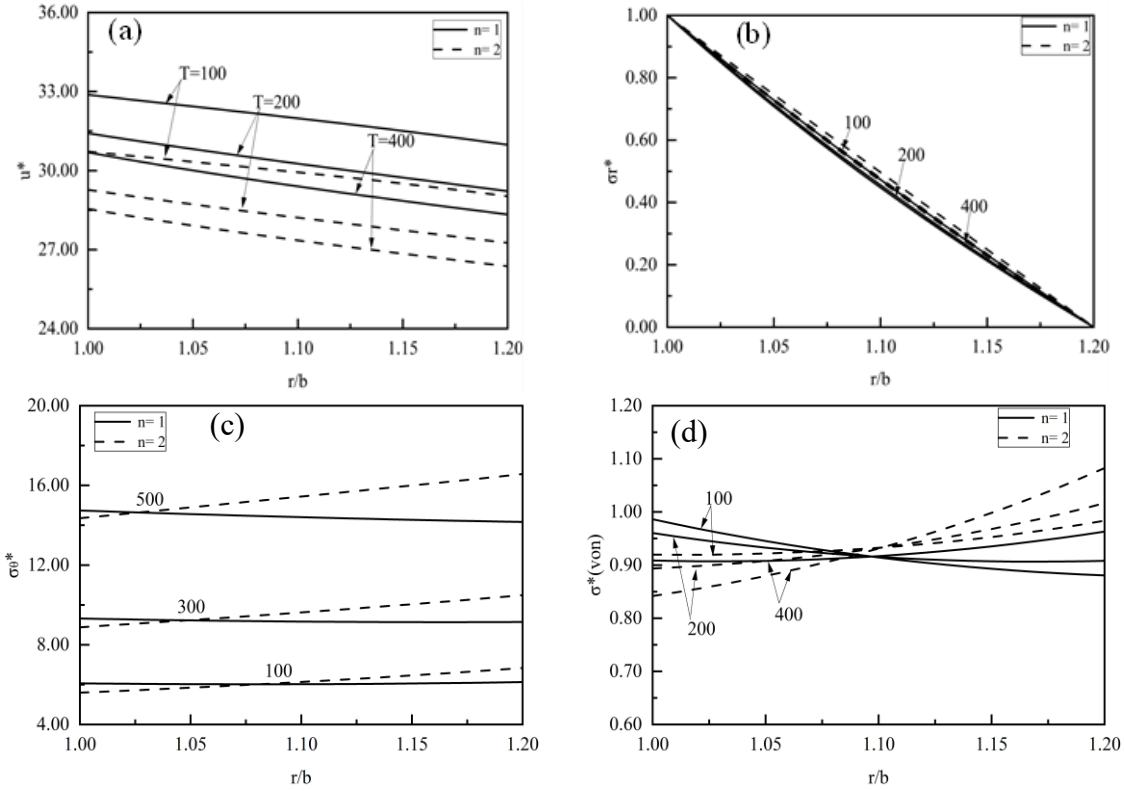

Fig. 5 Effect of temperature on displacement and stresses for internal pressure case

stress, tangential stress, and von Mises stress, respectively, for an internally pressurized (50 MPa) cylinder. The magnitude of displacement and radial stress is inversely related to the temperature, as shown in the figure for both ***n*** = 1 & 2 because increasing the temperature softens the material, which influences and reduces the radial stress and increases radial deformation. But in the case oftangential stress and von Mises stress, the magnitude of both is inverse concerning to temperature up to ***r/b*** = 1.09, then this relation is proportional onwards because up to the critical value of the radius, the temperature is less pronounced, due to this, the dominant effect is less. Beyond the critical radius, the tangential stress is more influenced by temperature, resulting in higher tangential and von Mises stress.

5.4 Effect of various pressure (internal pressure)

Fig. 6(a-d) shows the effect of various pressures (50, 100, 200) on displacement, radial stress, tangential stress, and von Mises stress, respectively, for an internally pressurized cylinder. The magnitude of displacement, radial stress, and von Mises stress is proportionally related to the pressure that represents the linear elastic behavior where stress is directly proportional to the strain, but tangential stress is inversely related to pressure, as shown in the figure because increasing pressure leads to radial expansion that decreases the tangential stress, this critical response is important to understand the failure modes under various pressures. The critical value of ***n*** with respect to the radius is shifting outward when increasing the internal pressure.

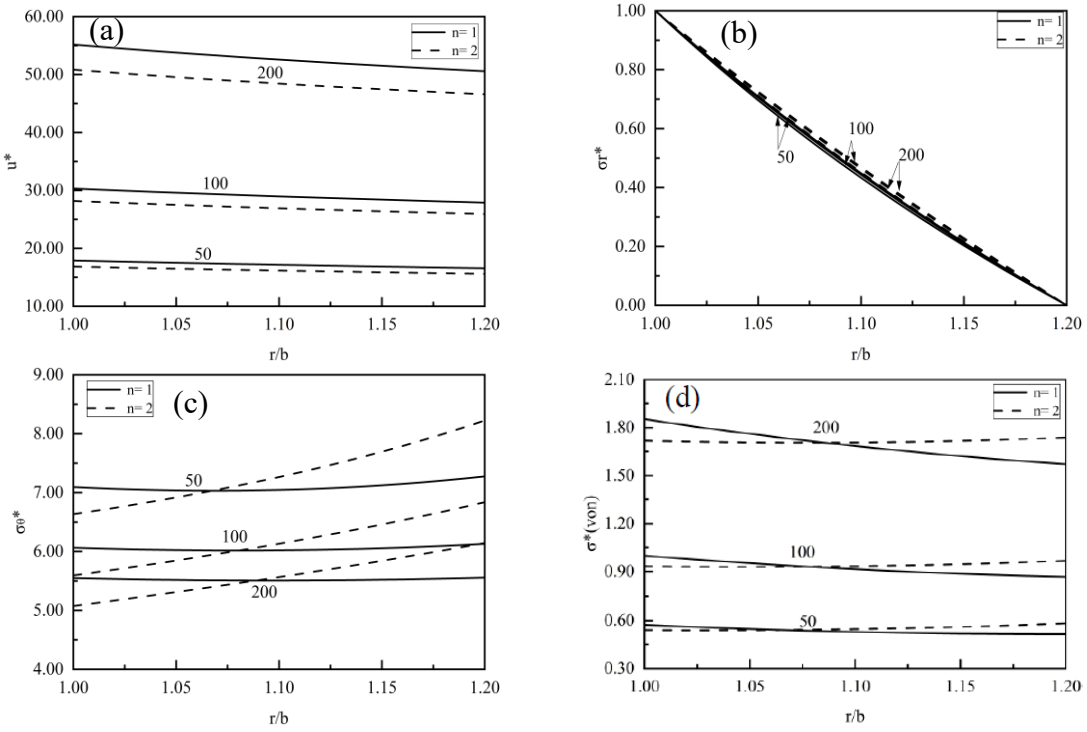

Fig. 6 Effect of various pressure on displacement and stresses for internal pressure case

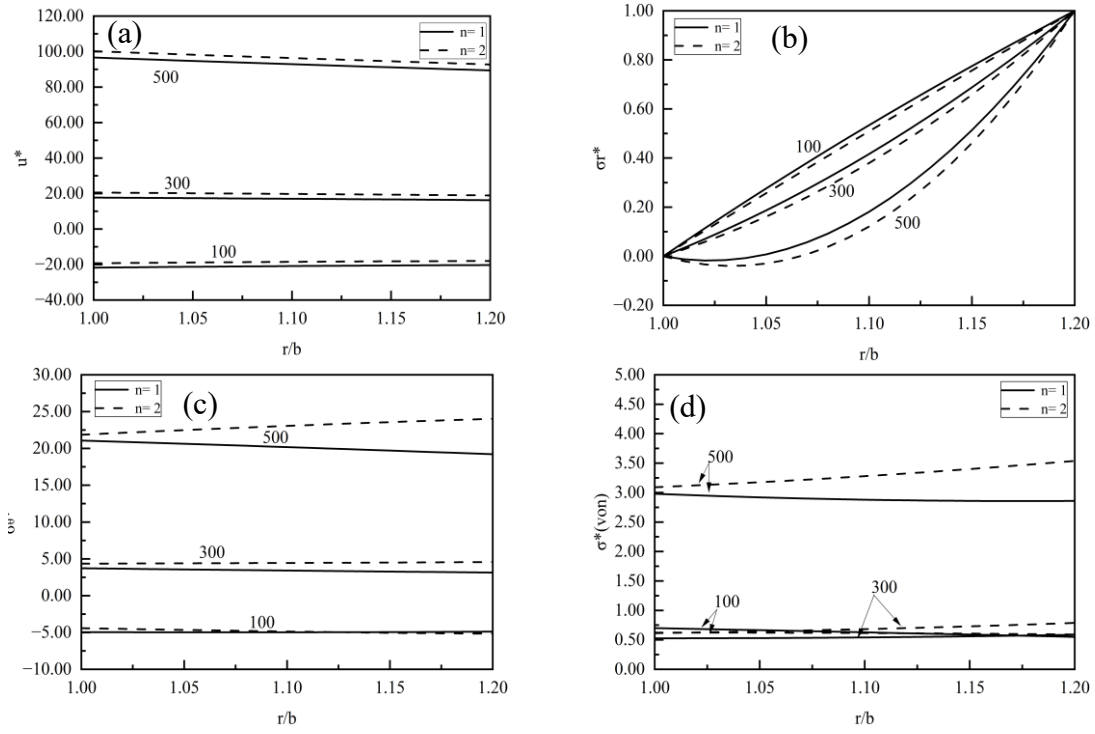

Fig. 7 Effect of various rotations on displacement and stresses for external pressure case

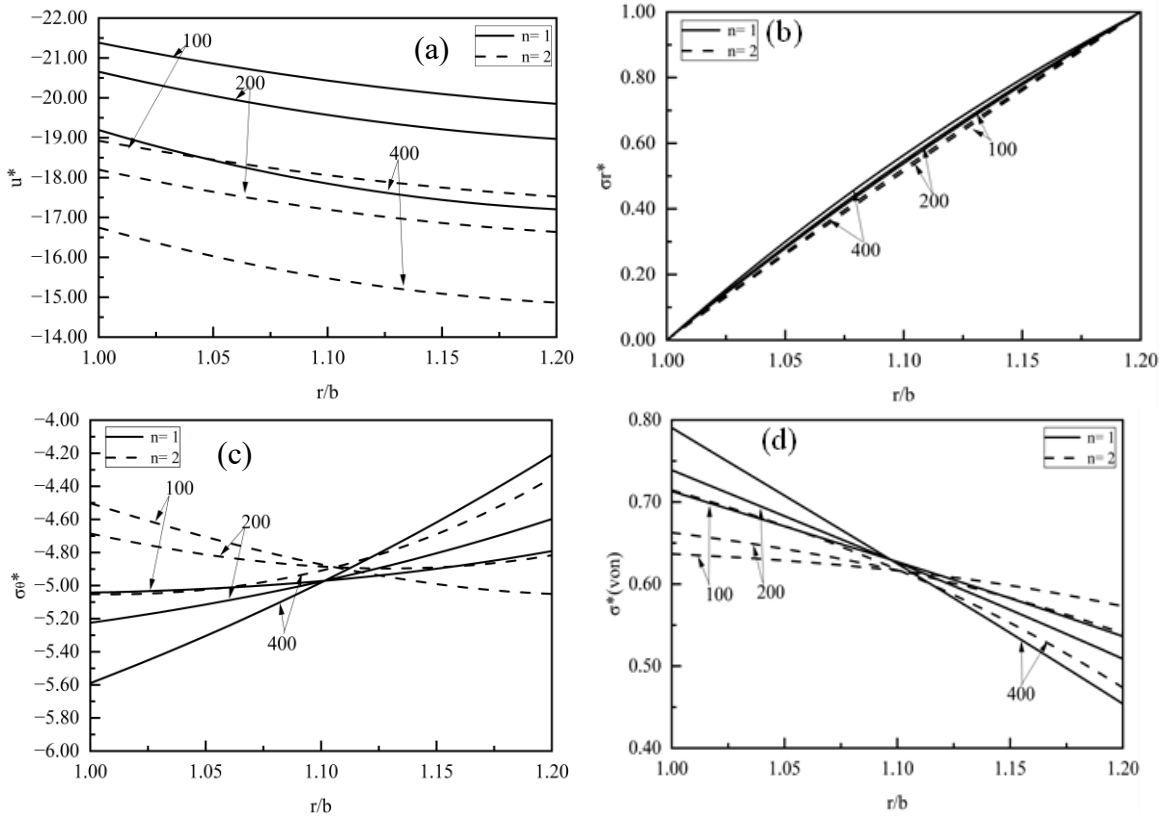

Fig. 8 Effect of various temperatures on displacement and stresses for external pressure case

5.5 Effect of various rotations (external pressure)

Fig. 7(a-d) shows the effect of various rotations (100, 300, 500) on displacement, radial stress, tangential stress, and von-Mises stress respectively for externally pressurized (100 MPa) cylinder. The magnitude of displacement and tangential stress is proportionally related to rotation for $\boldsymbol{n}$ = 1 & 2. However, radial stress is inversely related to rotation because centrifugal force increases with an increase in rotation that reduces the net compressive force due to the external pressure. This conflict of opposite radial and tangential stress relation with rotation results in von Mises stress distribution is clearly shown.

5.6 Effect of various temperature (external pressure)

Fig. 8(a-d) shows the effect of various temperatures (100, 200, 400) on displacement, radial stress, tangential stress, and von Mises stress, respectively, for an externally pressurized (100 MPa) cylinder. In the case of an externally pressurized cylinder, the displacement is inversely proportional to the temperature because increasing the temperature, the material generally expands, but external pressure exhibits compression. The material exhibits reduced resistance to displacement due to the combined effects making it more easily deformable. The influence of $\boldsymbol{n}$ is clearly observed in the

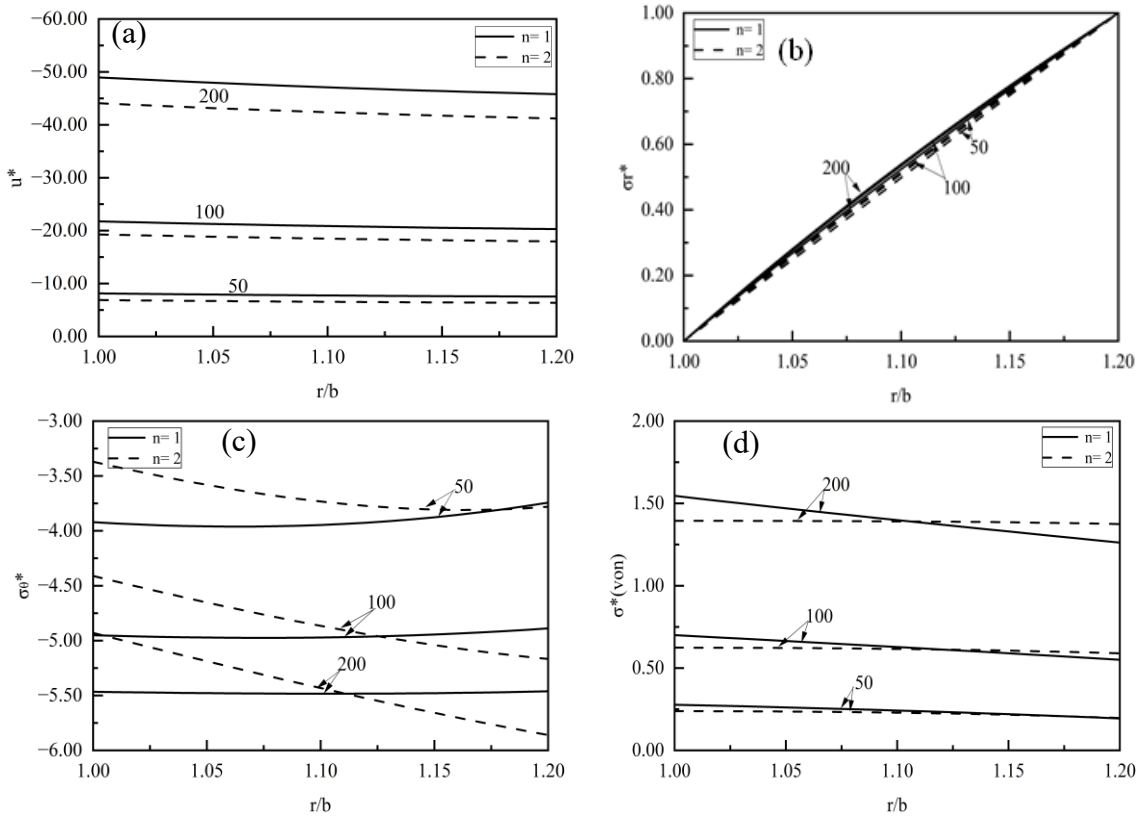

Fig. 9 Effect of various pressure on displacement and stresses for external pressure case

figure. The magnitude of radial stress is directly proportional to temperature across the thickness, as it depends on the material's ability to resist radial pressure. Similarly, tangential stress and von Mises stress also show a direct relationship with temperature, converging up to approximately ***r/b***=1.10. Beyond this point, the relationship becomes inversely proportional, causing the stresses to diverge toward the outer radius.

5.7 Effect of various pressure (external pressure)

Fig. 9(a-d) shows the effect of various pressures (50, 100, 200 MPa) on displacement, radial stress, tangential stress, and von Mises stress for an externally pressurized cylinder. The magnitude of displacement and stresses increases with the increase of external pressure for both ***n*** = 1 & 2 because the increase in external pressure imposes higher compressive forces. This proportional relation is also justified by the classical mechanics principles that material behaves elastically under a specified pressure range. The critical value of the converging-diverging point in tangential stress shifts towards the inner surface as the external pressure increases, whereas in von Mises stress, this critical value shifts towards the right when the external pressure increases because the dominant stress components are changing at this critical point. The material yielding is more pronounced in the case of increasing external pressure.

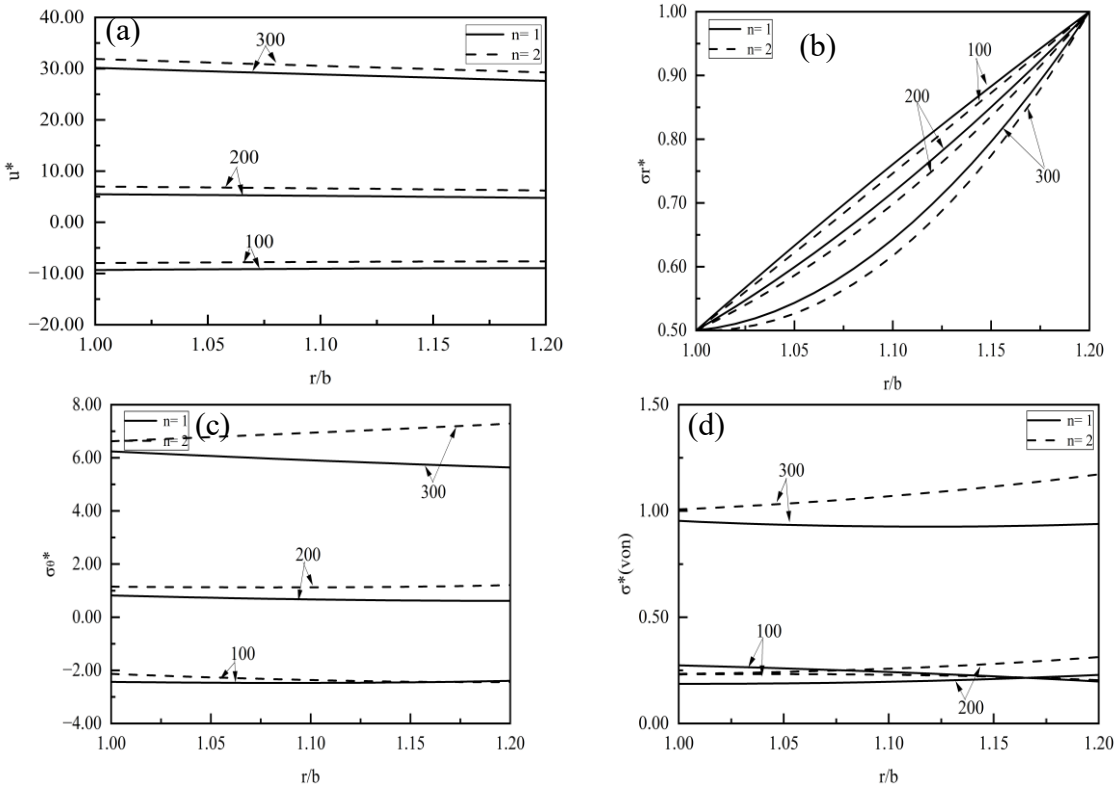

Fig. 10 Effect of various rotations on displacement and stresses for combined internal and external pressure case

5.8 Effect of various rotations (internal and external pressure)

Fig. 10(a-d) shows the effect of various rotations (100, 200, 300) on displacement, radial stress, tangential stress, and von Mises stress, respectively, for both internally (50 MPa) and externally (100 MPa) pressurized cylinders. The magnitude of displacement and tangential stress is directly proportional to the rotation for both $\boldsymbol{n}$ = 1 & 2, because a higher value of angular rotation generates higher centrifugal forces, and the magnitude for $\boldsymbol{n}$ = 2 is higher than the magnitude of $\boldsymbol{n}$ = 1. In the case of radial stress, the magnitude of radial stress is inversely proportional to rotation because the compressive force of external and internal pressures is reduced due to the increase in centrifugal force and is higher for $\boldsymbol{n}$ = 1 as compared to $\boldsymbol{n}$ = 2. Because of the opposite relation of radial stress and tangential stress with rotation, the effect of this conflict is shown in von Mises stress distribution for w = 100 & 200.

5.9 Effect of various temperatures (internal and external pressure)

Fig. 11(a-d) shows the effect of various temperatures (50, 100, 300) on displacement, radial stress, tangential stress, and von Mises stress, respectively, for both internally (50 MPa) and externally (100 MPa) pressurized cylinders. Displacement is reduced with the increase of temperature, whereas radial stress is directly proportional to the temperature because the ability of

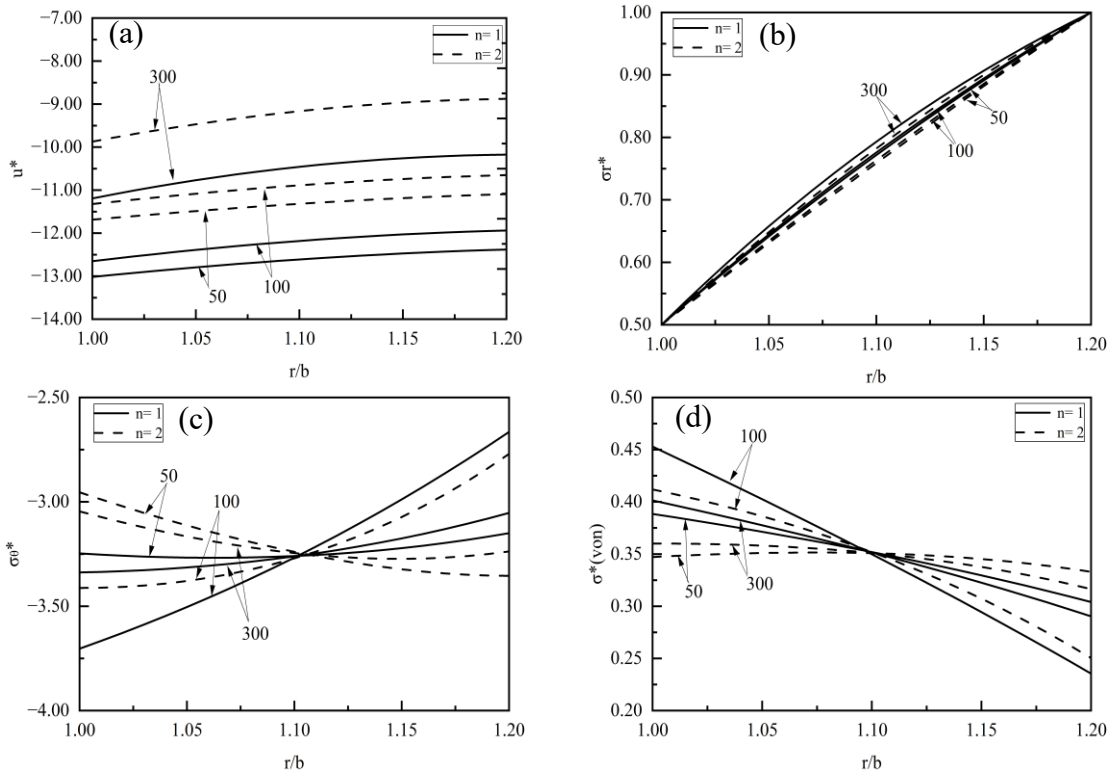

Fig. 11 Effect of various temperatures on displacement and stresses for combined internal and external pressure case

material to withstand radial stress is increased with temperature rise, as is the material's ability to resist compressive force due to pressure better at higher temperatures. Tangential and von Mises stress are first converging up to ***r/b***=1.10 (approx.), then diverging because the material's response is more uniform near the inner region, whereas the outer region may experience different responses as compared to the inner region. The converging to diverging behavior could be due to softer material at outer layers at alleviated temperature. The magnitude of tangential stress and von Mises stress increases from T = 50 to T = 100 but decreases for T = 300 in the converging region, but the trend is reversed in the diverging region.

5.10 Effect of various pressure (internal and external pressure)

Fig. 12(a-d) shows the effect of various pressures (100, 200, 300 MPa) on displacement, radial stress, tangential stress, and von Mises stress, respectively, for both internally and externally pressurized cylinders. The magnitude of displacement, tangential stress, and von Mises stress is increased with pressure because of an increase in elastic deformation leading to higher noticeable responses, but the magnitude of radial stress is decreased with pressure because outward centrifugal force is balanced by compression force. When increasing the pressure, the convergence point in the case of tangential stress is shifting outward, indicating that the dominating tensile effect is due to higher pressure, but shifting inward in von Mises stress due to the complex condition between radial and tangential stresses.

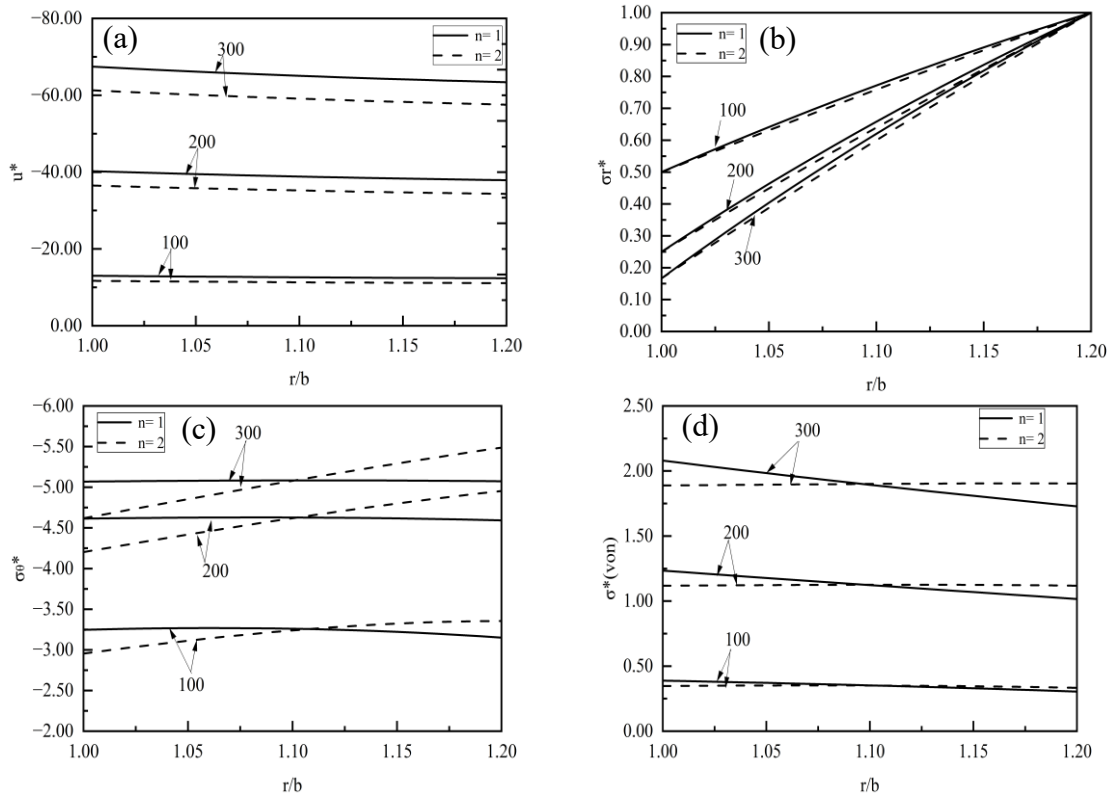

Fig. 12 Effect of various pressure on displacement and stresses for combined internal and external pressure case

6. Conclusions

This study presents an exact thermo-mechanical analytical solution for a functionally graded (FG) cylindrical pressure vessel subjected to complex loading conditions. The analysis considered for varying material properties governed by power law distribution, while assuming a constant Poisson's ratio. Thermo-mechanical elastic stresses were obtained for free-free boundary conditions by employing the Navier's method to solve the governing differential equation under plane stress conditions. The influence of the non-homogeneity constant, angular rotation, temperature variation, and internal and external pressures on displacement and stress distribution was investigated. The key findings from this study are summarized as follows:

• Radial Stress Behavior: Under internal pressure, the radial stress becomes zero at the outer surface, under external pressure, it is zero at the inner surface. When both internal and external pressures are applied simultaneously, the radial stress is nonzero on both boundaries. In all scenarios, the radial stress remains tensile throughout the vessel wall, confirming the critical influence of pressure boundary conditions.

• Impact of Material Gradation: The variation of material properties across the radial direction significantly influences both displacement and stress distribution. This demonstrates the importance of selecting appropriate gradation parameters to optimize structural performance, especially in environments involving thermal and mechanical coupling.

• Design Implications: The insights gained from this analytical investigation serve as a valuable reference for engineers and designers working with cylindrical FG structures. The results facilitate informed decision-making regarding the selection of gradation profiles and loading configurations to enhance structural integrity, reliability, and service life under multi-physics environments.

Overall, this work contributes a robust analytical framework for evaluating FG cylindrical vessels, offering both theoretical insight and practical relevance in advanced structural applications across aerospace, mechanical, civil, and energy systems.

References

Abbas, E.N., Njim, E.K., Jweeg, M.J., Madan, R., Ogaili, A.A.F. and Al-Maliky, F.T. (2025), "Experimental and theoretical analysis of mechanical properties of composite materials with diverse reinforcement types", *World J. Eng*., ahead-of-print, https://doi.org/10.1108/WJE-07-2024-0433.

Adiga, K., Herbert, M.A., Rao, S.S. and Shettigar, A. (2022), "Applications of reinforcement particles in the fabrication of Aluminium Metal Matrix Composites by Friction Stir Processing - A Review", *Manuf. Rev*., **9**, 26. https://doi.org/10.1051/mfreview/2022025

Allam, O., Draiche, K., Bousahla, A.A., Bourada, F., Tounsi, A., Benrahou, K.H., Mahmoud S.R., Adda Bedia E.A. and Tounsi, A. (2020), "A generalized 4-unknown refined theory for bending and free vibration analysis of laminated composite and sandwich plates and shells", *Comput. Concr*., **26**(2), 185-201. https://doi.org/10.12989/cac.2020.26.2.185

Alhous, Z.F.A., Jweeg, M.J., Njim, E.K., Mouthanna, A., Flayyih, M.A., Madan, R., Khobragade, P. and Rai, P.K. (2025), "Nonlinear frequency and dynamic response of PLA polymeric imperfect FG sandwich plates under hygrothermal conditions", *Coupled Syst. Mech*., **14**(1), 119. https://doi.org/10.12989/csm.2025.14.1.001

Al-Shablle, M., Njim, E.K., Jweeg, M.J. and Al-Waily, M. (2023), "Free vibration analysis of composite face sandwich plate strengthens by Al2O3 and SiO2 nanoparticles materials", *Diagnostyka*, **24**(2), 1-9.

Bayat, M., Sahari, B.B., Saleem, M., Ali, A. and Wong, S.V. (2009), "Bending analysis of a functionally graded rotating disk based on the first order shear deformation theory", *Appl. Math. Modell*., **33**(11), 4215-4230. https://doi.org/10.1016/j.apm.2009.03.001

Boss, J.N. and Ganesh, V.K. (2006), "Fabrication and properties of graded composite rods for biomedical applications", *Compos. Struct*., **74**(3), 289-293. https://doi.org/10.1016/j.compstruct.2005.04.030

Dai, H.L. and Fu, Y.M. (2006), "Magnetothermoelastic stress in orthotropic hollow cylinders due to radially symmetric thermal and mechanical loads", *Struct. Eng. Mech*., **24**(6), 699-707. https://doi.org/10.12989/SEM.2006.24.6.699

Daneshmand, S., Vini, M.H., Sajadi, S.M., Mouthanna, A., Jasim, D.J., Hammoodi, K.A., Hekmatifar, M. and Nasajpour-Esfahani, N. (2023), "Numerical and experimental investigations of mechanical, tribological, and electrical properties of laminated Bi-metal Al/SiC/Ni composites", *Mater. Today Commun*., **37**, 107355. https://doi.org/10.1016/j.mtcomm.2023.107355

Draiche, K., Bousahla, A.A., Tounsi, A. and Hussain, M. (2021), "An integral shear and normal deformation theory for bending analysis of functionally graded sandwich curved beams", *Arch. Appl. Mech*., **91**(12), 4669-4691. https://doi.org/10.1007/s00419-021-02005-0

Draiche, K., Tounsi, A., Ibrahim, K.D. and Tlidji, Y. (2024), "An improved mathematical model for static and dynamic analysis of functionally graded doubly-curved shells", *Arch. Appl. Mech*., **94**(6), 1589-1611. https://doi.org/10.1007/s00419-024-02595-5

Ellali, M., Amara, K. and Bouazza, M. (2024), "Thermal buckling of porous FGM plate integrated surface-bonded piezoelectric", *Coupled Syst. Mech*., **13**(2), 171-186. https://doi.org/10.12989/CSM.2024.13.2.171

Garg, A., Belarbi, M.O., Li, L., Chalak, H.D., Tounsi, A. and Zenkour, A.M. (2024), "Comparative study on the buckling analysis of exponential, power and sigmoidal sandwich FGM plates under hygro-thermal conditions", *Adv. Mater. Res*., **13**(6), 431-462. https://doi.org/10.12989/AMR.2024.13.6.431

Hadji, L., Bernard, F., Safa, A. and Tounsi, A. (2021), "Bending and free vibration analysis for FGM plates containing various distribution shape of porosity", *Adv. Mater. Res.*, **10**(2), 115-135. https://doi.org/10.12989/amr.2021.10.2.115

Hashemi, S. and Jafari, A.A. (2020), "An analytical solution for nonlinear vibrations analysis of functionally graded plate using modified lindstedt-poincare method", *Int. J. Appl. Mech.*, **12**(1), 2050003. https://doi.org/10.1142/S1758825120500039

Jabbari, M., Bahtui, A. and Eslami, M.R. (2009), "Axisymmetric mechanical and thermal stresses in thick short length FGM cylinders", *Int. J. Press. Vessel Pip.*, **86**(5), 296-306. https://doi.org/10.1016/j.ijpvp.2008.12.002

Jabbari, M., Sohrabpour, S. and Eslami, M.R. (2002), "Mechanical and thermal stresses in a functionally graded hollow cylinder due to radially symmetric loads", *Int. J. Press. Vessel Pip.*, **79**(7), 493-497. https://doi.org/10.1016/S0308-0161(02)00043-1

Kadum Njim, E., Al-Maamori, M.H., Madan, R., Bakhy, S.H., Al-Waily, M., Khobragade, P. and Hadji, L. (2024), "Numerical and analytical investigation of free vibration behavior of porous functionally graded sandwich plates", *Mech. Adv. Compos. Struct.*, **12**(3), 555-568. https://doi.org/10.22075/macs.2024.34962.1710

Kumar, A. and Kumar, D. (2021), "Vibration analysis of functionally graded stiffened shallow shells under thermo-mechanical loading", *Proceedings of the International Conference on Advances in Materials Processing & Manufacturing Applications*, **44**, 4590-4595. https://doi.org/10.1016/j.matpr.2020.10.826

Madan, R. and Bhowmick, S. (2020), "A review on application of FGM fabricated using solid-state processes", *Adv. Mater. Proc. Technol.*, **6**(3), 608-619. https://doi.org/10.1080/2374068X.2020.1731153

Madan, R. and Bhowmick, S. (2022), "Material modelling and limit angular speed analysis of porous trigonometric functionally graded rotating disk", *Adv. Mater. Proc. Technol.*, 1-13. https://doi.org/10.1080/2374068X.2022.2036043

Madan, R., Saha, K. and Bhowmick, S. (2020), "Limit speeds and stresses in power law functionally graded rotating disks", *Adv. Mater. Res.*, **9**(2), 115-131. https://doi.org/10.12989/AMR.2020.9.2.115

Madenci, E., Gulcu, S. and Draiche, K. (2024), "Analytical nonlocal elasticity solution and ANN approximate for free vibration response of layered carbon nanotube reinforced composite beams", *Adv. Nano Res.*, **16**(3), 251-263. https://doi.org/10.12989/anr.2024.16.3.251

Mahmoud Hosseini, S. (2014), "Elastic wave propagation and time history analysis in FG nanocomposite cylinders reinforced by carbon nanotubes using a hybrid mesh-free method", *Eng. Comput.*, **31**(7), 1261-1282. https://doi.org/10.1108/EC-12-2012-0312

Najibi, A. and Shojaeefard, M.H. (2016), "Elastic mechanical stress analysis in a 2D-FGM thick finite length hollow cylinder with newly developed material model", *Acta Mechanica Solida Sinica*, **29**(2), 178-191. https://doi.org/10.1016/S0894-9166(16)30106-9

Nejad, M.Z., Jabbari, M. and Ghannad, M. (2015), "Elastic analysis of axially functionally graded rotating thick cylinder with variable thickness under non-uniform arbitrarily pressure loading", *Int. J. Eng. Sci.*, **89**, 86-99. https://doi.org/10.1016/j.ijengsci.2014.12.004

Raad, H., Najim, E., Jweeg, M., AlWaily, M., Hadji, L. and Madan, R. (2024), "Vibration analysis of sandwich plates with hybrid composite cores combining porous polymer and foam structures", *J. Comput. Appl. Mech.*, **55**(3). https://doi.org/10.22059/jcamech.2024.377658.1121

Rabia, B., Tahar, H.D. and Abderezak, R. (2024), "Interfacial stresses in porous PFGM-RC hybrid beam", *Adv. Mater. Res.*, **13**(1), 37-53. https://doi.org/10.12989/AMR.2024.13.1.037

Rahimi, G.H., Arefi, M. and Khoshgoftar, M.J. (2011), "Application and analysis of functionally graded piezoelectrical rotating cylinder as mechanical sensor subjected to pressure and thermal loads", *Appl. Math. Mech.*, **32**(8), 997-1008. https://doi.org/10.1007/s10483-011-1475-6

Rahimi, G.H., Arefi, M. and Khoshgoftar, M.J. (2012), "Electro elastic analysis of a pressurized thick-walled functionally graded piezoelectric cylinder using the first order shear deformation theory and energy method", *Mechanika*, **18**(3), 292-300. https://doi.org/10.5755/j01.mech.18.3.1875

Safari, A., Tahani, M. and Hosseini, S.M. (2011), "Two-dimensional dynamic analysis of thermal stresses in a finite-length FG thick hollow cylinder subjected to thermal shock loading using an analytical method",

Acta Mechanica, **220**(1-4), 299-314. https://doi.org/10.1007/s00707-011-0478-y
Sondhi, L., Sahu, R.K., Kumar, R., Yadav, S., Bhowmick, S. and Madan, R. (2023), "Functionally graded polar orthotropic rotating disks: Investigating thermo-elastic behavior under different boundary conditions", *Int. J. Interact. Des. Manuf.*, **18**(1), 159-166. https://doi.org/10.1007/s12008-023-01447-w
Suresh, S. and Mortensen, A. (1997), "Functionally graded metals and metal-ceramic composites: Part 2 Thermomechanical behaviour", *Int. Mater. Rev.*, **42**(3), 85-116. https://doi.org/10.1179/imr.1997.42.3.85
Tutuncu, N. and Temel, B. (2009), "A novel approach to stress analysis of pressurized FGM cylinders, disks and spheres", *Compos. Struct.*, **91**(3), 385-390. https://doi.org/10.1016/j.compstruct.2009.06.009
Wang, Y.Q. and Zhao, H.L. (2019), "Free vibration analysis of metal foam core sandwich beams on elastic foundation using Chebyshev collocation method", *Arch. Appl. Mech.*, **89**(11), 2335-2349. https://doi.org/10.1007/s00419-019-01579-0
Wang, Y. and Wu, D. (2017), "Free vibration of functionally graded porous cylindrical shell using a sinusoidal shear deformation theory", *Aerosp. Sci. Technol.*, **66**, 83-91. https://doi.org/10.1016/j.ast.2017.03.003
Wang, Z.W., Zhang, Q., Xia, L.Z., Wu, J.T. and Liu, P.Q. (2015), "Stress analysis and parameter optimization of an fgm pressure vessel subjected to thermo-mechanical loadings", *Procedia Eng.*, **130**, 374-389. https://doi.org/10.1016/j.proeng.2015.12.230
Zine, A., Tounsi, A., Draiche, K., Sekkal, M. and Mahmoud, S.R. (2018), "A novel higher-order shear deformation theory for bending and free vibration analysis of isotropic and multilayered plates and shells", *Steel Compos. Struct.*, **26**(2), 125-137. https://doi.org/10.12989/scs.2018.26.2.125

CC